energies

MDPI

Article

Study on Impulse Breakdown Characteristics of Internal-Gap Lightning Protection Device Applied to 35 kV Distribution Line

Zhen Fang [1,2], Bowen Wang [1,2,*], Jiazheng Lu [1,2] and Zhenglong Jiang [1,2]

1 State Key Laboratory of Disaster Prevention & Reduction for Power Grid Transmission and Distribution Equipment, Changsha 410129, China; policy@139.com (Z.F.); lujz1969@163.com (J.L.); jiangzhenglong0518@126.com (Z.J.)

2 State Grid Hunan Electric Power Company Disaster Prevention and Reduction Center, Changsha 410129, China

* Correspondence: bowen_wm@163.com; Tel.: +86-0731-8633-2057

Received: 2 June 2018; Accepted: 29 June 2018; Published: 4 July 2018

Abstract: External environmental factors have no effect on the breakdown performance of the internal gap, leading to the anti-icing and anti-storm features of the internal-gap lightning protection device (ILPD). In this paper, a test platform is created to study the impulse discharge and arc erosion characteristics of the ILPD applied to a 35 kV distribution line. The 50% lightning impulse voltage and discharge stability of the ILPD are experimentally analysed. The results show that the ILPD has good discharge voltage repeatability under multiple impulses. Under a positive lightning impulse, the 50% breakdown voltage of the ILPD is 3.8–11.4% higher than that of the outer-gap lightning protection device (OLPD). A finite element simulation model is created for electric field analysis. The maximum electric field strength of the ILPD is 4.68% lower than that of the OLPD, leading to a higher lightning breakdown voltage. High-speed camera shooting shows that the discharge arc may lead to the erosion of the discharge tube, reducing its insulation performance. A large current impulse test platform is set up for arc energy analysis, which indicates that more than 90% of the energy is absorbed by the varistor during lightning stroke. The quality and leakage current of the discharge tube did not change significantly after testing. Given the current design of varistors, the per unit length energy of arc is less than 4.5 J/mm due to the numerical calculation, which is far less than the experimental arc energy (25.0 J/mm). Therefore, arc erosion will not cause the insulation performance of discharge tube to decrease when using the current varistor design.

Keywords: internal-gap; lightning protection; lightning impulse voltage; arc; high-speed camera; varistor

1. Introduction

The internal-gap lightning protection device (ILPD) and outer-gap structure lightning protection device (OLPD) are two different types of lightning protection device. When the lightning striking distribution line does not have a lightning protection device, power outages occur easily, which may lead to arc burn of the insulator surface and wire breaking [1,2]. Surge arresters with series gap are being wildly applied to protect insulation to prevent flashovers and circuit interruptions, especially for covered distribution lines [1]. To decrease the difficulty of transmission line reconstruction and prevent the need for insulation coordination with the insulator, an anti-lightning composite insulator that combines the arrester and insulator was developed to be applied to distribution lines [3]. Most of the above reconstruction methods use an outer-gap structure lightning protection device (OLPD). Compared with no-gap structure protection devices, the outer-gap lightning protection device can

prevent the varistor from aging and reduce the leakage current and residual voltage, so these devices are being widely used in power systems. However, the structure of the outer-gap is easily affected by the external environment [4]. Under harsh environments such as rainstorms, the discharge gap is prone to bridging by rain, leading to malfunction of lightning protection device.

In early 2008 in Central Southern China, an ice storm caused more than 120,000 power line towers to collapse, more than 7000 electrical lines fell, and 859 substations shut down according to the statistic provided by the South Power Grid Corp of China. Iced-covered insulator flashover was one of the main reasons for the power outages [5]. During icing, the outer-gap lightning protection device becomes prone to icing bridge, so the outer insulation of the anti-ice design is a critical aspect of the outer-gap structure.

Additionally, overvoltage is common in distribution lines. Sudden changes in an electric network cause transient phenomena to occur. These transient events result in the creation of an overvoltage or of a high-frequency periodic or oscillating wave train with rapid damping. These changes include breaking of small inductive currents, re-arcing, phase-to-earth faults, and so on. The ratio of the surge voltage to the rated voltage may reach four under these situations [6]. Metal oxide lightning protection devices are much more sensitive to overvoltage than insulators, so as the frequency energy continues to pour into the internal ZnO varistor, the aging of varistor accelerates.

The internal-gap was proposed to address the above problems, while maintaining the advantages of the outer-gap. The breakdown characteristics of the gap are not affected by external environmental factors. The internal-gap lightning protection device (ILPD) has been widely used in distribution systems in Japan [7]. During the discharge process, the gas in the internal-gap is not connected with the outside air, leading to the difference in the impulse breakdown characteristics compared with the outer-gap. The impulse discharge characteristics of internal-gap have been investigated. Delliou et al. reported that the discharge homogenously propagated in the whole tube when the inner radius is below 300 μm, discharges propagated with a tubular shape when the inner radius was around 300 μm, and propagated as classical streamers for larger inner diameters. The distance between electrode and the dielectric and electrode spacing were critical parameters influencing the discharge characteristics [8]. Pai et al. studied the transitions between corona, glow, and spark regimes of nanosecond repetitively pulsed discharges at atmospheric pressure in air preheated from 300 K to 1000 K. The research indicated that a glow-like regime exists when the atmospheric-pressure air was preheated to relatively high temperatures [9,10]. Srivastava and Zhou analyzed surface charge accumulation under impulse voltage. This research explained why some insulators that can be charged by direct current (DC) voltage cannot be charged by impulse voltage, no matter how high the amplitude of the voltage [11]. Bouazia indicated that a high arc current will act on the surface material of the discharge tube. When the material absorbing the heat of the arc reaches a certain value, some of the bonds in the macromolecular chain will be broken. If the temperature is too high, the material is directly vaporized to form a low molecular gas product, affecting the insulation properties of the surface material of the discharge tube [12]. The above research methods are summarized in Appendix A.

The study of the impulse discharge characteristics of the internal-gap are being focused on the discharge tube itself. Whereas the ILPD is a discharge tube in series with the ZnO varistor, the electric field distribution and the arc energy are quite different from the simple discharge tube due to the presence of the varistor. The discharge characteristics of the ILPD have been less studied. In this paper, a lightning impulse test platform is built to study the impulse discharge characteristics of the ILPD to examine its characteristics under multiple lightning strikes and the 50% lightning impulse discharge voltage of the ILPD. A finite element simulation model is set up to investigate the difference in the discharge characteristics of ILPD and OLPD. A high-speed camera is used to study the arc movement in the gap. A large current impulse test is performed to analyse the insulation properties of the surface material of the discharge tube under high arc current. Based on the experimental research and simulation analysis, the theoretical basis for ILPD design is provided.

2. Experimental Platform and Sample

The ILPD needs to perform reliably under lightning strikes, so the discharge characteristics of the internal-gap under lightning strikes need to be studied. The experimental platform for lightning impulse voltage is shown in Figure 1. The test power was the impulse voltage generator, with a rated voltage of 400 kV. The main capacitor was charged to the set voltage. Then the circuit was automatically triggered by the spark gap to form a positive polarity lightning discharge voltage of 1.2/50 μs. The environment temperature and humidity were 23.5 °C and 53%, respectively.

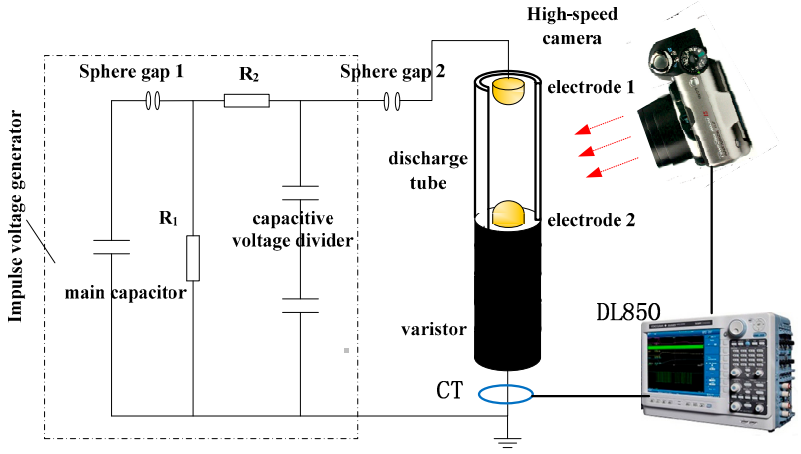

Figure 1. Test circuit of impulse voltage.

The up-and-down test method was used in the experiment [13]. The time interval between the two impulses was a charging time of 70 s. The next test value was determined by the last test phenomenon. If the last test resulted in withstand, the next voltage was increased by 5%. Otherwise, the next test voltage value was decreased by 5%. When the two last test phenomena were different (from withstand to flashover or vice versa), the following tests were defined as useful tests. The 50% lightning breakdown voltage (V_{50}) is the average value of the useful tests.

$$V_{50} = \frac{\sum_{1}^{N} U_i}{N} \tag{1}$$

where U_i is the voltage value of the useful test and N is the total number of useful tests. For each gap distance, 30 useful tests were carried out. In the tests, a high-speed camera (Photron Fastcam SA-5 (Photron, Tokyo, Japan)) was used to record arc discharge in the discharge tube. The time interval between two frames was 6.6 μs and the exposure time of each photo was 0.369 μs. Discharge current waveforms were acquired with a Pearson 4418 (Pearson Electronics, Palo Alto, CA, USA) and Yokogawa DL850E oscilloscope (Yokogawa Electric Corporation, Tokyo, Japan), which also functioned as the trigger signal for the high-speed camera.

The ILPD sample of the lightning impulse experiment is shown as Figure 2. The OLPD sample was the ILPD sample without the discharge tube. The discharge tube was made of epoxy material (CY 1300, density 1.16 g/cm^3), widely used in lightning protection devices [7] with a relative permittivity of 3.5. The inner and outer diameters of the discharge tube were 50 and 60 mm, respectively. Epoxy material was replaced by transparent glass to enable the observation of the arc operation of the ILPD. The discharge electrodes were hemispherical electrodes, as shown in Figure 2. The reference voltage of the varistor was 66 kV, meeting the standard requirements for 35 kV lightning protection device [14]. The 50% lightning discharge voltage was experimentally analysed under gap distances ranging from 180 to 240 mm.

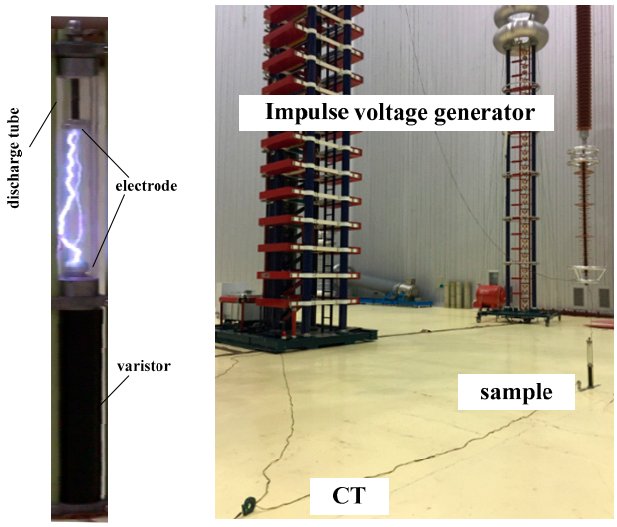

Figure 2. Experimental sample and platform: (**a**) the internal-gap lightning protection device (ILPD) sample and (**b**) the experimental platform.

3. Experimental Results

3.1. Experimental Waveform and Discharge Stability

The typical voltage and current waveforms under a 200 mm internal-gap distance are shown in Figure 3. The result show that the current passing through the sample under the lightning voltage impulse was less than 1 kA.

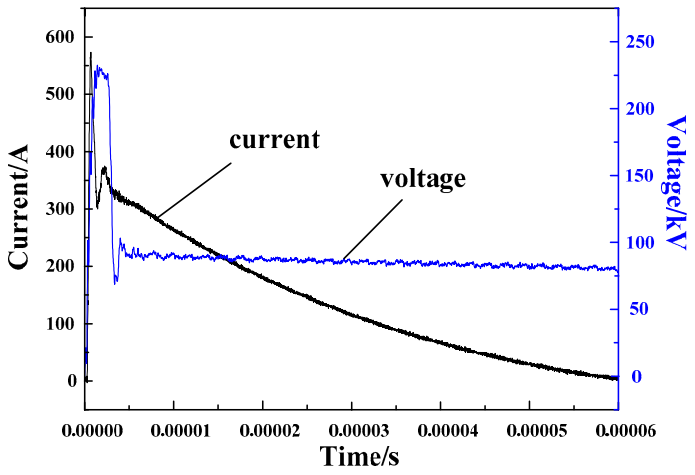

Figure 3. Typical waveforms of voltage and current.

According to the up-and-down test method, the 30 useful values of the lightning impulse discharge voltage in OLPD and ILPD are shown in Figure 4. The results show that the repeatability of the discharge voltage of ILPD is good under a discharge time interval of 70 s. The relative average deviations of the lightning impulse voltage in ILPD and OLPD were 3.16% and 3.73% respectively, which are very close.

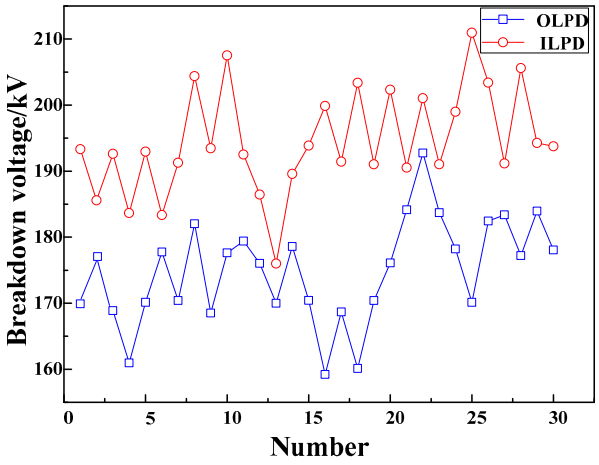

Figure 4. Lightning impulse voltage variation.

3.2. Expeimental of Lightning Impulse Voltage

The results for the 50% impulse breakdown voltage of ILPD and OLPD under different electrode distances are shown in Table 1. According to Table 1, the discharge voltage increased with increasing gap distance. Under the positive lightning impulse, the breakdown voltage of the ILPD was 3.8–11.4% higher than that of the OLPD. When the gap distance of the ILPD increased from 180 mm to 240 mm, the breakdown voltage increased from 173 kV to 212 kV, respectively. According to the standard requirements, the 50% positive polarity lightning impulse voltage of the 35 kV lightning protection device with a series gap was less than 240 kV [14]. The results show that the gap distance of 240 mm meets the standard requirements. The empirically derived equation for ILPD and OLPD with different gap distances (l) is proposed to predict the 50% breakdown voltage U. The equations are shown in Equations (2) and (3), respectively. Compared with the OLPD, the breakdown voltage of the ILPD increased overall, as shown in Figure 5.

$$U_1 = 4.95l^{0.69} \tag{2}$$

$$U_2 = 4.68l^{0.69} \tag{3}$$

where the gap distance l is in millimeters and the 50% breakdown voltage U is in kilovolts.

Table 1. Test data of impulse voltage.

Gap Distance (mm)	U_1/kV	U_2/kV	Relative Deviation
180	173	166	3.80%
200	194	174	11.40%
220	203	189	7.03%
240	212	202	4.95%

4. Theoretical Analysis

Experimental results showed that the ILPD discharge stability is good. Under positive lightning impulses, the breakdown voltage of the ILPD was 3.8–11.4% higher than that of the OLPD. The electric field distribution had an important influence on the development of the streamer development. When the discharge tube was present, the electric field distribution of the gap changed. Appling finite element analysis, the electric field distribution of the gap was analysed. The dielectric physical parameters of the insulator are shown in Table 2. Two assumptions were proposed here: (1) the applied voltage was 10 kV and (2) in the simulation, an artificial boundary was established so that the distance

from the lightning protection device to the boundary was much greater than the length of the lightning protection device itself. The potential on the boundary was assumed to be zero. The simulation model is provided in Figure 6 and the electric field distribution in the simulation is shown in Figure 7.

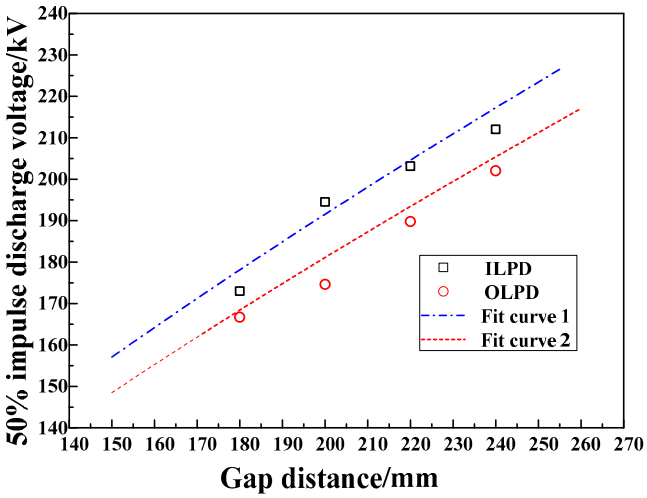

Figure 5. The results of impulse voltage experiment.

Table 2. Physical parameters of the dielectric materials.

Dielectric	Relative Permittivity	Conductivity (μS/cm)
Air	1	0
Metal	10^8	5.998×10^7
ZnO	600	10^{-10}
Discharge tube	3.5 or 10	10^{-12}

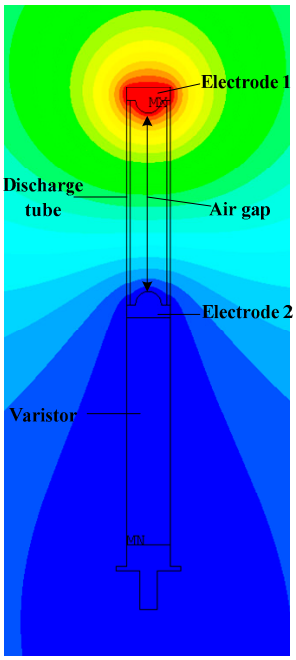

Figure 6. The electric field simulation of the internal gap structure. MX is the maximum potential, where the voltage is applied. MN is the minimum potential, where is contact with the earth.

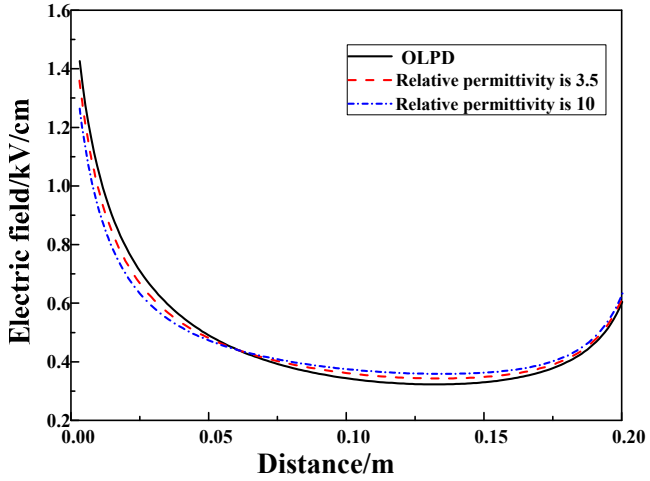

Figure 7. The results of electric field simulation.

The simulation results indicate that the maximum electric field strength of the ILPD is 4.68% lower than that of the OLPD and the maximum electric field strength decreases with increasing relative permittivity of the discharge tube. When the relative permittivity of the discharge tube increased from 3.5 to 10, the maximum electric field strength decreased from 136 kV/m to 126 kV/m and the deviation compared to the maximum electric field strength of the OLPD increased from 4.68% to 11.90%.

According to the streamer theory [15,16], the streamer starts at a position near the electrode where the ionization coefficient is equal to the adhesion coefficient under a positive DC voltage. In the development of an electron avalanche moving to the positive electrode, the charge of the head of the electron avalanche increases. When the total amount of charges in the head of the electron avalanche are greater than the critical charge number, the streamer starts. The critical charge number is generally considered to be 10^8. The beginning of the streamer needs to meet two conditions under positive polarity impulse voltage: (1) the applying voltage of the electrode or the electric field at the tip of the electrode must reach the minimum voltage U_0 or field strength E_0 required at the initial period of the streamer under the impulse of voltage, and (2) effective free electrons in the electrode head must be ensured. The simulation results show that the existence of a discharge tube reduces the maximum field strength of the gap. Therefore, applying a higher impulse voltage is necessary to reach the initial streamer voltage, leading to a higher breakdown voltage in the ILPD higher than in the OLPD, as shown in Table 1.

In addition, when a positive polarity lightning current is applied to the ILPD, the surface of the discharge tube accumulates the charge, and the decay can last for hours [11,17]. Therefore, the discharge tube accumulates charge, affecting the breakdown characteristics of the gap. Wang inferred that micro-discharge or corona discharge is a prerequisite for charge accumulation. In the absence of micro-discharge or corona discharge conditions, the accumulated charge is small due to a simple gap or creeping breakdown flashover, leading to a dielectric surface voltage of less than 0.5 V [18]. Lightning impulse voltage breakdown process is transient, no corona and micro-discharge phenomenon appearing. The influence of the charge accumulation of the discharge tube surface on the breakdown voltage can be neglected.

Therefore, the main reason for the difference in the 50% impulse breakdown voltage between ILPD and OLPD is the change in electric field distribution due to the presence of the discharge tube.

5. Discussion

A high-speed camera (Photron Fastcam SA-5) was used to record arc discharge in the discharge tube, as shown in Figure 8. Experimental results show that the randomness of the discharge arc can cause the arc to move along the surface of the discharge tube. If the arc energy is large enough,

the surface material is ablated, affecting the discharge tube insulation. If the insulation of the discharge tube is damaged, the power frequency voltage applied directly to the ZnO varistor accelerates the aging of the ZnO varistor, finally leading to the failure of the ILPD. However, the difference between the lightning impulse test energy and the actual lightning current energy is large, so that simulating the actual erosion condition of the lightning current along the surface under the above experimental analysis is impossible. In this paper, a large current impulse test platform was built for an arc erosion experiment.

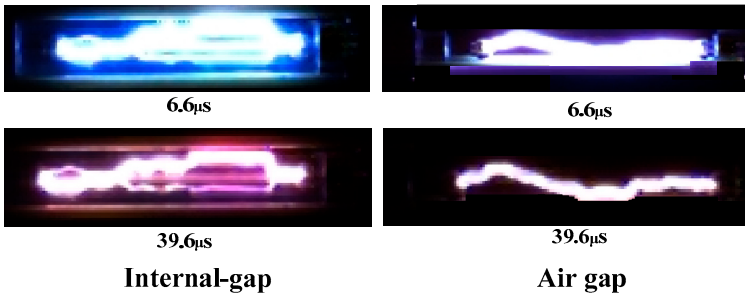

Figure 8. Photos obtained with the high-speed camera.

The high current impulse experimental circuit is shown in Figure 9. In the figure, C is the discharge capacitor, T is the thyristor working as the discharge switch, D paralleled with T is an inverse diode, and L_s and R_s are the total inductance and resistance in the discharge circuit, respectively. When the capacitor was charged to a preset voltage U_0, the thyristor T was triggered to conduct. Two high-voltage probes (Tektronix P6015 (Tektronix, Beaverton, OR, USA)) measured the voltage waveforms at the upper and lower electrodes of the discharge tube under high current impulse, with a probe ratio of 1000:1. The waveform of the current was measured using a Pearson 4418. The current and voltage parameters were recorded with a Yokogawa DL850E oscilloscope.

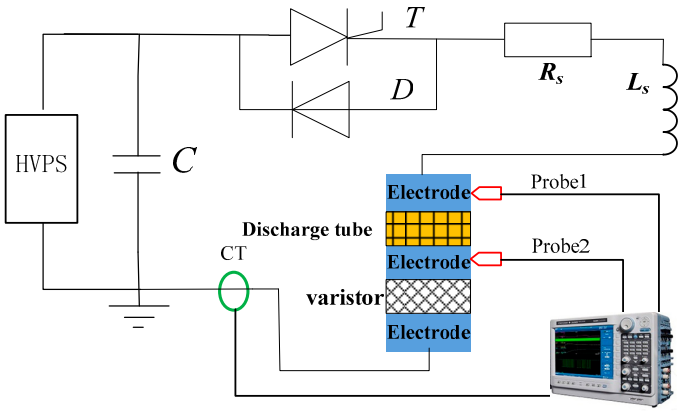

Figure 9. The high current impulse circuit.

The simulated discharge tubes were the discharge tube shortened in length. The height of the simulated discharge tube was 10 mm for easy flashover under low voltage. The inner and outer diameters were the same as those in Figure 2. The DC 1 mA voltage of the varistor was 4 kV, which was designed according to the compression ratio of the simulated discharge tube. In order to simulate the arc moving along the discharge tube surface, the electrode surface was parallel to the upper and lower surfaces of the discharge tube. The simulated discharge tube was subjected to an 8/20 μs impulse test, with a magnitude ranging from 5.64 kA to 25.94 kA. Ten simulated discharge tubes made of epoxy material were prepared for testing. Each simulated discharge tube was tested 10 times.

The surface leakage current of sample under DC or alternating current (AC) voltage and quality changes in the atmospheric environment are the main parameters for the arc erosion study of traditional insulation material [19,20]. A 0.1 mg resolution for the high-precision electronic scales was used for quality measurement. The DC leakage current was measured using a Keithley 6517B (Tektronix, Beaverton, OR, USA). The environment temperature and humidity were 26.5 °C and 63%, respectively.

The typical voltage and current waveforms are shown in Figure 10. The experimental results are shown in Table 3, where W_t is the total energy flowing through the discharge tube and the varistor, W_a is the arc energy inside the simulated discharge tube, and η is the ratio of W_a to W_t, as shown in Figure 11. The experimental results indicate that the W_a and W_t increased with increasing current. η was almost consistent under different currents ranging from 4.82% to 6.23%. Therefore, more than 90% of the energy was absorbed by the varistor during lightning strike and the proportion of arc energy was small.

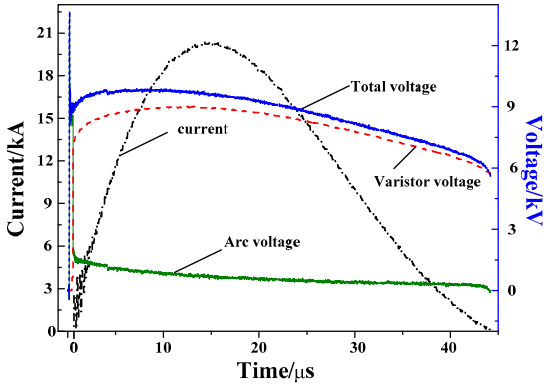

Figure 10. Typical waveforms of voltage and current.

Table 3. Experimental results.

Current (kA)	W_t (J)	W_a (J)	η (%)
5.64	1050.34	55.99	5.33
12.85	2230.54	138.86	6.23
19.57	3466.73	167.12	4.82
25.94	4653.42	250.18	5.38

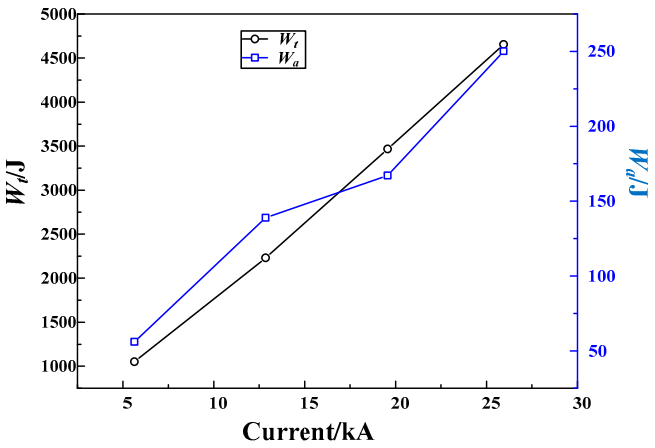

Figure 11. The relationship between energy and current.

Comparing before and after testing, the quality of the simulated discharge tube did not change significantly. The change in mass was less than 0.1% within measurement error. The inner surface leakage current under a 3000 V DC voltage was measured before and after testing. The leakage current and surface resistivity under different arc energy are shown in Figure 12. The results indicate that the leakage current increases and the surface resistivity decreases when the arc energy is larger than 138.86 J. However, the leakage current was below 50 nA and the surface resistivity was larger than 1×10^{15} W·cm after testing, which means that the insulation performance of the discharge tube did not significantly degrade and an arc energy blow 250.18 J did not ablate the discharge tube.

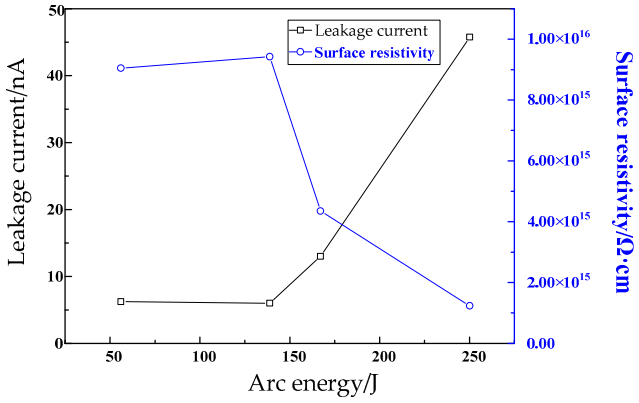

Figure 12. The leakage current and surface resistivity under different arc energy.

Whether the energy of the test was enough to match the energy of a lightning current was analysed theoretically. The V-I (voltage and current) curve of the ZnO varistor of a 35 kV ILPD is shown in Figure 13. The V-I curve was divided into three sections: small current area, middle current area, and high current area. The piecewise function was applied to fit the three sections. The fitting expression of the V-I characteristic function in each area are shown as follows:

$$\begin{array}{l} u = 12.048i^{0.1172}, i \le 10^{-3} \\ u = 5.400i^{0.0436}, 10^{-3} < i \le 500 \\ u = 4.2639i^{0.0858}, 500 < i \end{array} \quad (4)$$

where u (kV) is the maximum voltage when the current i (A) flows through the ZnO varistor. According to the standard requirements [14], a 35 kV lightning protection device with a series gap must pass the 4/10 μs waveform high-current impulse test twice with 65 kA amplitude. For computational convenience, a 4/10 μs high current impulse of 65 kA amplitude is represented by a simplified bevel pulse wave, which is shown as follows:

$$i = \begin{cases} 16250 \times 10^6 t & (0 < \mathrm{t} \le 4\mu s) \\ -5420 \times 10^6 t + 86720 & (4\mu s < \mathrm{t} \le 16\mu s) \end{cases} \quad (5)$$

where t is time (s). As the pulsed current duration (microsecond level) is negligible in comparison with the thermal time constants of the materials surrounding the ZnO varistor (the ZnO thermal diffusivity $a_z = 0.7 \times 10^{-7}$ m^2/s, the aluminum thermal diffusivity $a_{Al} = 8.61 \times 10^{-5}$ m^2/s) [21,22], the discharge process can be considered adiabatic for the ZnO varistor. Therefore, heat dissipation can be ignored in the calculation. The energy w absorbed by the ZnO varistor under a single impulse current is provided by Equation (6):

$$w = \int uid\mathrm{t} \quad (6)$$

The total energy passing through the ZnO varistor with a 4/10 μs high current with a 65 kA amplitude was calculated to be 69 kJ. Based on the ratio of the arc energy test, the arc energy was approximately 2.97 kJ.

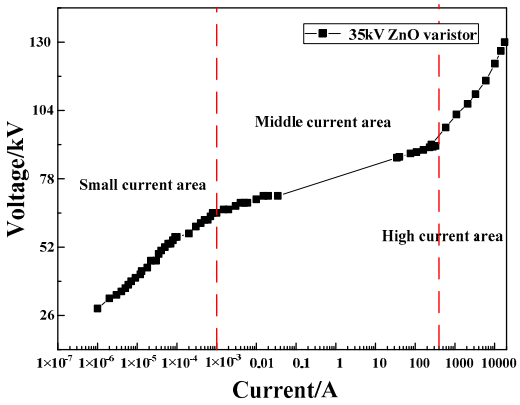

Figure 13. The voltage-current (V-I) curve of the ZnO varistor.

According to the theoretical analysis, the arc energy of the ILPD reached 2.97 kJ with the through-flow capacity design of the ZnO varistor. In order to facilitate the analysis, the following assumptions were made: (1) the overall gap length of the ILPD was 220 mm and (2) the arc ablates the discharge tube along the surface, and the arc energy is the same everywhere.

Therefore, the arc energy per unit length along the surface was less than 4.5 J/mm. In this paper, the impulse energies of the high current impulse test were all larger than 4.5 J/mm and the maximum energy reached 25.0 J/mm, which is much larger than the design requirements. In addition, the test time of the simulated discharge tube was 10, which is a worse arc impulse than the standard requirements. Therefore, given the design of the current capacity of the ZnO varistor of the ILPD, the arc will not degrade the insulation performance of the discharge tube.

6. Conclusions

In this paper, the impulse discharge characteristics of the ILPD applied to a 35 kV distribution line was studied. We drew the following conclusions:

(1) The lightning impulse discharge voltage experiment results showed that the repeatability of the discharge voltage of ILPD is good under a discharge time interval of 70 s.

(2) Under a positive lightning impulse, the breakdown voltage of the ILPD was 3.8–11.4% higher than that of the OLPD. The simulation results indicated that when the relative permittivity of discharge tube increased from 3.5 to 10, the maximum electric field intensity decreased from 136 kV/m to 126 kV/m, and the deviation compared to the maximum electric field strength of the OLPD increased from 4.68% to 11.90%, leading to a higher breakdown voltage for the ILPD.

(3) Based on the images captured by the high-speed camera, if the arc energy is sufficiently large, the surface material will be ablated, affecting the discharge tube insulation.

(4) In this paper, a large current impulse test platform was built for an arc erosion experiment. The result indicated that more than 90% of the energy was absorbed by the varistor during lightning strike. The change in mass after testing decreased by less than 0.1% within measurement error. The leakage current was below 50 nA and the surface resistivity was larger than 1×10^{15} W·cm after testing, which means that an arc energy below 250.18 J does not ablate the discharge tube.

(5) In this paper, the impulse energy of the high current impulse test reached 25.0 J/mm, which is much larger than the design requirement of 4.5 J/mm. Therefore, given the current capacity

design of the ZnO varistor of the ILPD, the arc will not degrade the insulation performance of the discharge tube.

Author Contributions: Z.F. and B.W. conceived the idea for this work. B.W. performed the experiments and mathematical analysis. B.W. contributed to the manuscript text and figures. J.L. and Z.J. designed and supervised all the work, analysed and discussed the data results, and prepared the manuscript.

Funding: The State Grid Corporation of China Science and Technology Program (5216AF160005).

Conflicts of Interest: The authors declare no conflict of interest.

Appendix A

Table A1. The synthesis of the solutions proposed in the literature [8–12].

Authors	Solutions
Delliou et al.	The discharge characteristic of discharge tube are analyzed through the method of discharge experimental under different electrode spacing and different distance between electrode and dielectric.
Pai et al.	The transitions between corona, glow and spark regimes of nanosecond repetitively pulsed discharge in the discharge tube were studied at atmospheric pressure in air preheated from 300 K to 1000 K.
Srivastava and Zhou	The surface charge accumulation under impulse voltage analyzed by measuring the charge after the impulse test.
Bouazia et al.	The insulation properties of surface material under the high arc current are analyzed by measuring the change of mass and the leakage current.

References

1. Washino, M.; Fukuyama, A.; Kito, K.; Kato, K. Development of current limiting arcing horn for prevention of lightning faults on distribution lines. *IEEE Trans. Power Deliv.* **1988**, *3*, 187–196. [CrossRef]
2. Chen, W.; Gu, S.; He, J.; Yin, B. Development of Arc-Guided Protection Devices Against Lightning Breakage of Covered Conductors on Distribution Lines. *IEEE Trans. Power Deliv.* **2010**, *25*, 196–204. [CrossRef]
3. Wang, B.W.; Lu, J.Z.; Fang, Z.; Jiang, Z.L.; Peng, Y.J.; Hu, J.P.; Wu, W. Study on Insulation Design and Lightning Protection Performance of Lightning Protection Composite Insulators for 10 kV Distribution Line. *Power Syst. Technol.* **2018**, *42*, 2001–2008. (In Chinese)
4. Lu, J.; Xie, P.; Hu, J.; Jiang, Z.; Fang, Z. AC Flashover Performance of 10 kV Rod-Plane Air-Gapped Arresters under Rain Conditions. *Energies* **2018**, *11*, 1563. [CrossRef]
5. Farzaneh, M.; Baker, A.C.; Bemstorf, R.A.; Chemey, E.A.; Chisholm, W.A.; Gorur, R.S.; Grisham, T.; Gutman, I.; Rolfseng, L.; Stewart, G.A. Selection of Line Insulators with respect to Ice and Snow, Part I: Context and Stresses. A position paper prepared by the IEEE Task Force on icing performance of line insulators. *IEEE Trans. Power Deliv.* **2007**, *22*, 2289–2296. [CrossRef]
6. Abdelhay, A.S.; Malik, O.P. *Protection of Electric Distribution Systems*; Wiley-IEEE Press: New York, NY, USA, 2011.
7. Hitoshi, S.; Katsuhiko, S.; Hiroyuki, K. Distribution Surge Arrester Failures due to Winter Lightning and Measurement of Energy Absorption Capability of Arresters. *IEEE Trans. Power Energy* **2012**, *132*, 554–559.
8. Delliou, P.L.; Tardiveau, P.; Jeanney, P.; Bauville, G.; Pasquiers, S. Development of pulsed discharges inside narrow cavities and their interaction with dielectric surfaces. In Proceedings of the 30th International Conference on Phenomena in Ionized Gases (ICPIG), Belfast, Northern Ireland, UK, 28 August–2 September 2011; p. C10.
9. Pai, D.Z.; Lacoste, D.A.; Laux, C.O. Transitions between corona, glow, and spark regimes of nanosecond repetitively pulsed discharges in air at atmospheric pressure. *J. Appl. Phys.* **2010**, *107*, 093303. [CrossRef]
10. Pai, D.Z.; Stancu, G.D.; Lacoste, D.A.; Laux, C.O. Nanosecond repetitively pulsed discharges in air at atmospheric pressure: The spark regime. *Plasma Sources Sci. Technol.* **2010**, *19*, 065015. [CrossRef]
11. Srivastava, K.D.; Zhou, J. Surface Charging and Flashover of Spacers in SF6 under Impulse Voltages. *IEEE Trans. Electr. Insul.* **1991**, *26*, 428–442. [CrossRef]

12. Bouazia, M.; Raynal, G.; Razafinimanana, M.; Gleizes, A. An Experimental and theoretical study of the absorption of SF6 arc plasma radiation by cold SF6 gas. *J. Phys. D Appl. Phys.* **1996**, *29*, 2885–2891. [CrossRef]
13. Yin, F.; Jiang, X.L.; Farzaneh, M.; Hu, J.L. Electrical performance of 330-kV composite insulators with different shed configurations under icing conditions. *IEEE Trans. Dielectr. Electr. Insul.* **2015**, *22*, 3395–3404. [CrossRef]
14. IEC 60099-8:2017. *Surge Arresters—Part 8: Metal-Oxide Surge Arresters with External Gap (EGLA) for Overhead Transmission and Distribution Lines of A.C. Systems Above 1 kV*; International Electrotechnical Commission: Geneva, Switzerland, 2017.
15. Nasser, E.; Heiszler, M. Mathematical-Physical model of the streamer in nonuniform field. *J. Appl. Phys.* **1974**, *45*, 3396–3401. [CrossRef]
16. Khaled, M. New method for computering the inception voltage of a rod-plan gap in atmospheric air. *Proc. Inst. Electr. Eng.* **1975**, *122*, 107–110. [CrossRef]
17. Al-Bawy, I.; Farish, O. Charge Deposition on an Insulating Spacer under Impulse Voltage Conditions. *IEE Proc. A* **1991**, *138*, 145–152. [CrossRef]
18. Wang, F.; Qiu, Y.; Pfeiffer, W.; Kuffel, E. Insulator Surface Charge Accumulation under Impulse Voltage. *IEEE Trans. Dielectr. Electr. Insul.* **2004**, *11*, 847–854. [CrossRef]
19. Sarathi, R.; Rajesh Kumar, P.; Sahu, R.K. Analysis of surface degradation of epoxy nanocomposite due to tracking under AC and DC voltages. *Polym. Degrad. Stab.* **2007**, *92*, 560–568. [CrossRef]
20. Takahiro, I.; Fumio, S.; Toshiyuki, N.; Tamon, O.; Toshio, S.; Masahiro, K.; Toshikatsu, T. Effects of Nano- and micro-filler mixture on electrical insulation properties of epoxy based composites. *IEEE Trans. Dielectr. Electr. Insul.* **2006**, *13*, 319–326.
21. Picci, G.; Rabuffi, M. Pulse handling capability of energy storage metallized film capacitors. *IEEE Trans. Plasma Sci.* **2000**, *28*, 1603–1606. [CrossRef]
22. Lengauer, M.; Rubeša, D.; Danzer, R. Finite element modelling of the electrical impulse induced fracture of a high voltage varistor. *J. Eur. Ceram. Soc.* **2000**, *20*, 1017–1021. [CrossRef]